J. Fluid Mech. (1978), *vol.* 85, *part* 2, *pp.* 369–385
Printed in Great Britain

Velocity characteristics of the flow in the near wake of a disk

By D. F. G. DURÃO AND J. H. WHITELAW
Department of Mechanical Engineering, Imperial College, London

(Received 9 May 1977)

Measurements of the velocity characteristics of near-wake flows were obtained with a direction-sensitive laser-Doppler anemometer. The wakes were formed downstream of central disks of diameters 8·9, 12·5 and 14·2 mm which were located on the centre-line of a 20·0 mm jet. Detailed measurements were obtained with initial annular-jet velocities of from 9·4 to 39·5 m/s and include values of the axial and radial components of the mean velocity, the three normal stresses and the shear stress. Probability density distributions and energy spectra were also measured.

The results show, for example, that the curvature of the annular jet increases with disk diameter and that the ratios of the maximum positive and negative centre-line velocities to the exit velocity increase with decreasing disk diameter and are essentially independent of the initial velocity. The turbulent field is substantially anisotropic with a minimum turbulence intensity of around 30 % in the recirculation region; the locations of zero shear stress and zero mean velocity gradient are not coincident. The measured spectra reveal predominant frequencies in a small region of the outer-shear layer and in the vicinity of the jet exit; these discrete frequencies did not propagate downstream nor into the recirculation region.

1. Introduction

Available information on the velocity and turbulence characteristics of wake flows with recirculation is limited and the measurement accuracy often low. As a consequence, general conclusions on the characteristics of turbulent wakes are difficult to formulate with certainty. On the basis of the data of Carmody (1964) and the results of one supporting figure from the preliminary investigation of annular-jet flow by Durão & Whitelaw (1974), however, it was concluded by Pope & Whitelaw (1976) that the velocity profiles in the plane of a trailing edge have a considerable influence on downstream properties and that, in general, present turbulence models are unable to characterize near-wake flows. The incorrect representation of energy dissipation was identified as the most likely source of error in the turbulence models. Castro & Robins (1977), on the basis of their investigations of the flow around a cube, also suggested that present turbulence models are unable to characterize near-wake flows.

The present contribution is intended to provide more extensive knowledge of the velocity characteristics of near-wake flows with recirculation. The geometrical configuration is similar to that of Durão & Whitelaw (1974), whose preliminary measurements were carried out to evaluate instrumentation, and comprises a jet with carefully located central disks. This arrangement results in annular jet flows which are similar to

flame stabilizers used, for example, in small furnaces. A directionally sensitive laser-Doppler anemometer was used to determine the mean flow and turbulence characteristics of the corresponding wake flows, as a function of Reynolds number, with particular attention given to the region of recirculation immediately behind the disk. The results provide physical understanding of these wake flows and are reported in sufficient detail to allow a careful assessment of turbulence models of the type discussed by Pope & Whitelaw.

The investigation was motivated by the desire to calculate the properties of blunt-body stabilized flames and the knowledge that the various previous investigations, for example those of Longwell *et al.* (1949), Wohl, Kopp & Gazley (1949), Longwell (1953), Durão & Whitelaw (1976) and Clare *et al.* (1976), did not provide sufficient details on the aerodynamic properties of the recirculation region. The last two contributions, largely because of the availability of laser-Doppler anemometry, represent a significant improvement in that information on the local mean velocity and normal stress is reported. In preliminary attempts to calculate the properties of these various combusting flows, it was clear that the recirculation region and the subsequent wake decay were not well represented and that this failure stems in part from the turbulence model.

The present measurements include centre-line and radial distributions of the axial and radial components of the mean velocity and of the significant components of the stress tensor. Probability distributions of the three orthogonal components of the velocity vector and the skewness and flatness factors are reported where appropriate. Turbulence energy spectra corresponding to the axial component of velocity were obtained in an effort to determine the existence and magnitude of possible predominant frequencies.

The flow configurations and instrumentation are described briefly in the following section; details necessary to allow an assessment of the precision of measurement are provided. Section 3 presents and discusses the mean velocity characteristics of the flows and § 4 the related turbulence characteristics. A brief concluding discussion is also provided.

2. Equipment and instrumentation

The general arrangement of the annular-jet configuration is indicated on figure 1. It comprised an annular jet of diameter 20·0 mm with central disks of diameters 14·2, 12·5 and 8·9 mm. Detailed measurements were obtained with the largest disk and with a maximum jet exit velocity of 26·8 m/s; the influence of the initial velocity was investigated by obtaining measurements with values of 39·5, 26·8, 16·9 and 9·4 m/s.

The maximum and minimum Reynolds numbers, based on the annular-jet equivalent diameter, were $28{\cdot}3 \times 10^3$ and $3{\cdot}5 \times 10^3$ ($36{\cdot}2 \times 10^3$ and $5{\cdot}4 \times 10^3$ when based on disk diameter), and the flow contraction upstream of the exit, for the 14·2 mm diameter disk, was 50:1.

The measurements were obtained along the centre-line and along radii but only after the symmetry of the mean flow had been established by measuring profiles 90° apart at downstream distances corresponding to $x/D = 0$, 1 and 5 for each disk. The flow was accepted for further investigation if at the three downstream planes the mean profiles at each of the four sections agreed with each other to within 1 % of the maxi-

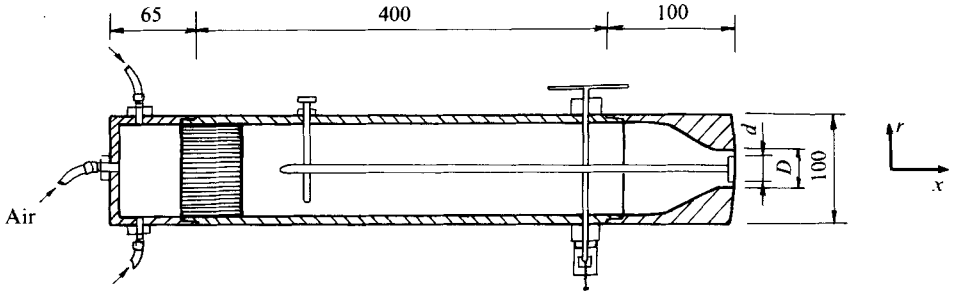

FIGURE 1. Annular-jet configuration. Dimensions in mm. U_0 = 39·5, 26·8, 16·9 or 9·4 m/s; D = 20·0 mm; d = 14·2, 12·5 or 8·9 mm; disks manufactured with sharp edges.

mum velocity in that plane. The annular jet was secured with its axis in the horizontal plane to an arrangement which allowed it to be traversed in three orthogonal planes and located, with respect to the measuring volume of the measuring instrumentation, within 0·05 mm.

The measurements were obtained with a laser-Doppler anemometer operating with forward-scattered light. The transmission arrangement comprised an argon laser (Spectra Physics Model 164) operating at a wavelength of 488 nm and powers around 100 mW and an integrated water-filled acousto-optic cell based on the earlier investigations of Durão & Whitelaw (1975). The acousto-optic cell provided two beams with a frequency difference of 30 MHz, which were separated to a parallel distance of 71 mm before being focused by a lens of diameter 100 mm and focal length 250 mm. The resulting intersection regions were, at the $1/e^2$ intensity locations, approximately 0·11 mm in diameter and 0·78 mm in length; the fringe spacing was 1·72 μm. Zero velocity and zero frequency corresponded to a measuring frequency and velocity of 30 MHz and $-51{\cdot}6$ m/s respectively. The light-collection system made use of a 70 mm effective diameter lens of focal length 150 mm and a 0·4 mm diameter pinhole located in front of a photomultiplier (EMI 9815B).

The resulting Doppler signals were processed either with a spectrum analyser (Hewlett-Packard model 8552A/8553B/141T) operating in a counting mode, as described by Durão, Laker & Whitelaw (1975), or with a frequency-tracking demodulator (Cambridge Consultants). The tracker was used to obtain energy spectra; high-pass filtering, amplification, mixing with a sine wave and subsequent filtering of the photomultiplier output signal allowed the demodulated signal to be spectrum analysed (General Radio Model 1564-A). Most results were obtained with the Hewlett-Packard analyser; the number of signals output from the instrument at linearly spaced centre-frequencies with constant bandwidth was observed at predetermined times to yield probability distributions of Doppler frequencies.

The errors associated with the optical arrangement stem mainly from the finite dimensions of the measuring volume and the consequent gradient-broadening effects. The light-collecting arrangement and the discrimination level of the electronic arrangements resulted in estimated effective control volumes of less than 0·10 mm in diameter and less than 0·70 mm in length and, using the analysis of Melling (1975), the influence on the mean velocity values was negligible. The tangential fluctuation measurements were the most influenced by gradient broadening but the maximum corresponding

error was not more than 3 %. An error in the value of the mean velocity may also arise from the subtraction of the shifted frequency from the measured frequency; thus the relative error in the vicinity of zero mean velocity is significant although its absolute value is negligible.

Errors associated with processing the Doppler signals by the present counter have been considered by Durão (1976) and can, in principle, arise from the number of counts, the observation of more fast-moving than slow-moving particles, the variation of signal quality with velocity and the finite filter width. In almost all the measurements, the number of counts exceeded that required to ensure errors of less than 1 % for mean and r.m.s. quantities, with a confidence interval of 95 %; the time between counts and the variation of signal quality with velocity are likely to ensure that the velocity bias effects are less than 1 % of the mean velocity; and the filter width was usually less than 1 % of the width of the Doppler spectrum. As a consequence, the great majority of mean and r.m.s. quantities are estimated to be subject to r.m.s. uncertainties of not more than 2 % and 4 % respectively.

The results with the counting arrangement were obtained without seeding the flow. Silicone-oil seeding was used to allow the use of the frequency-tracking demodulator. Significant errors from variations in particle number density are not likely in view of the previous findings of Baker (1974) and Durão & Whitelaw (1974).

Comments relating to the precision of the measurement of turbulence energy are introduced with the results.

3. Mean-velocity characteristics

Figure 2 presents centre-line values of the mean velocity normalized with the initial velocity for four values of the initial velocity and all three disks; the corresponding Reynolds numbers based on the hydraulic diameter of the annuli and on the disk diameters are given in the caption. Each flow has the same general characteristics: a region of recirculation where the mean velocity is negative, a region where the flow accelerates to a maximum velocity and a downstream region where the velocity decays.

It is clear that, for high Reynolds numbers and a given disk, the maximum and minimum non-dimensionalized mean velocities are essentially independent of the initial velocity and this suggests that the spreading rates are almost independent of the initial velocity. (For the two lower Reynolds number flows this does not apply, since the flow acceleration is slightly different.) The maximum and minimum velocities increase in magnitude with decreasing disk diameter as a direct consequence of the conservation of momentum. The spreading rate is not independent of the disk diameter as shown in table 1: the value of $\bar{U}_{\mathbb{C}_{\max}}/(\bar{U}_0 A)$, where A is the annular area, increases with d/D and implies an increased convergence of streamlines towards the centre-line, due to the decrease in the ratio of inertia to pressure forces in the wake behind the disks. Thus, although the length of the recirculation region increases with disk diameter, for a given initial velocity, its value decreases when normalized with the disk diameter. The initial velocity, at least at the higher Reynolds numbers, does not have a significant influence on the recirculation length although slightly larger lengths were noted for the lowest Reynolds number. In general, therefore, the disk diameter or annular gap influences the maximum and minimum velocities and the length of the recirculation

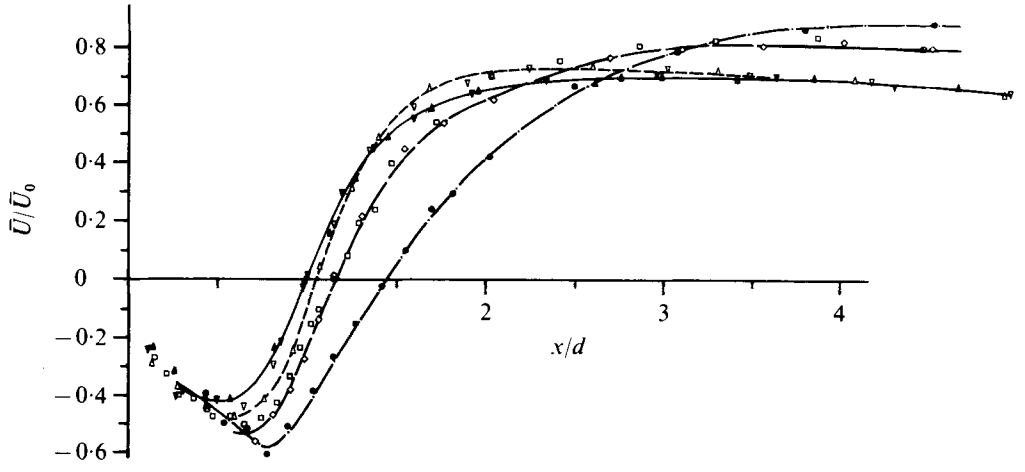

FIGURE 2. Centre-line profiles of the axial mean velocity in an annular jet. $D = 20$ mm.

	●	◇	□	▼	▲	▽	△
d (mm)	8·9	12·5	12·5	14·2	14·2	14·2	14·2
$\bar{U}_0$ (m/s)	39·5	39·5	26·8	39·5	26·8	16·9	9·4
x/d where $\bar{U}_{\mathbb{C}} = 0$	1·45	1·15	1·15	1·00	1·00	1·01	1·04
$Re_j \times 10^{-3} = [\bar{U}_0(D-d)/\nu] \times 10^{-3}$	28·3	19·1	13·0	14·8	10·0	6·3	3·5
$Re_d \times 10^{-3} = [\bar{U}_0 d/\nu] \times 10^{-3}$	22·7	31·8	21·7	36·2	24·5	15·5	8·6

d/D	$\bar{U}_{\mathbb{C}_{max}}/(\bar{U}_0 A)$ (mm^{-2})
0·445	$36{\cdot}1 \times 10^{-4}$
0·625	$43{\cdot}9 \times 10^{-4}$
0·710	$49{\cdot}6 \times 10^{-4}$

TABLE 1. Variation of maximum centre-line velocity with d/D.

region and confirms that, in the range of sizes considered, disk flame stabilizers with large diameters are likely to be more effective.

Radial profiles of the mean velocity were measured with the largest disk, which, according to figure 2, corresponds to smaller axial velocities and larger radial velocities. The measured values of the axial and radial components are plotted on figures 3 (*a*) and (*b*) for an initial velocity of 26·8 m/s. The measurements characterize the development of the flow in the wake of the disk and the profiles at $x/D = 6$ and 18·9 are essentially identical when normalized with the centre-line velocity and plotted against radial distance normalized with the width of the jet corresponding to the location of half the centre-line velocity; they are both identical to a fully developed free-jet profile and confirm the rapid development of the annular jet.

Isovels for the axial velocity are presented on figure 4, which also shows the rapid mixing of the flow and the small region of recirculation. Comparison of figures 3 (*a*) and (*b*) indicates that at $x/d = 0{\cdot}14$ the ratio of radial to axial velocity is around 0·07 in the region of the maximum axial velocity with higher values at other locations in the same plane. Pope & Whitelaw demonstrated that the calculation of downstream flow properties is particularly sensitive to the assumed initial profile of radial velocity and it

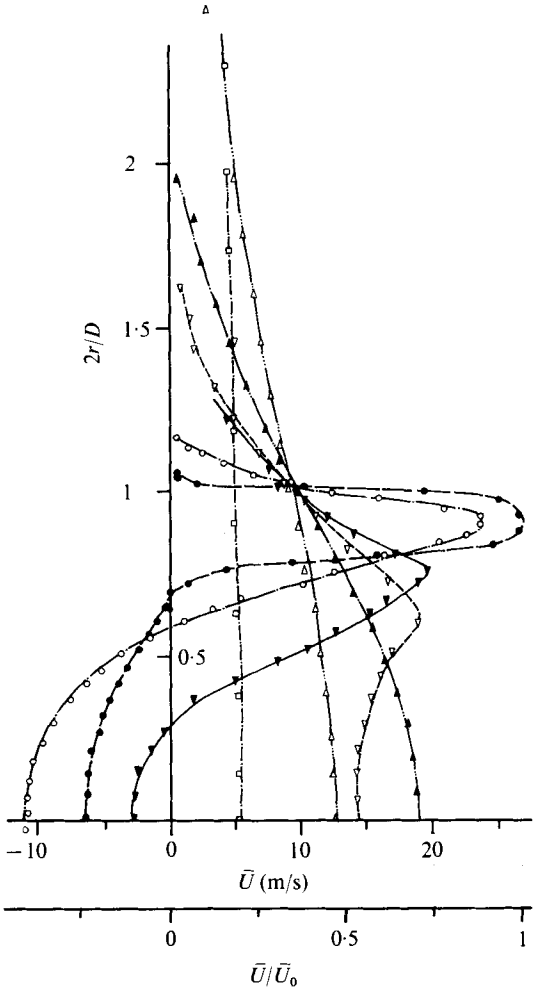

FIGURE 3(*a*). For legend see opposite.

can be expected that the neglect of the present finite radial velocities in any calculations would result in significant errors; however, use of the present measured values in the calculation method of Pope & Whitelaw may result in an even greater discrepancy between the measured and calculated regions of recirculation since the radial velocity is towards the centre-line. The rapid growth in the magnitude of the maximum radial velocity with downstream distance is consistent with the rapid spreading of the flow in the region where the centre-line values achieve a maximum negative value. The maximum radial velocity was measured at $x/d = 0{\cdot}42$ and corresponds to a ratio of radial to axial velocity of 0·73. Further downstream, and mainly after the centre-line mean velocities become positive, the radial velocities decay rapidly and are insignificant downstream of $1{\cdot}52d$.

The present results may be compared with those of previous authors. Since the experimental methods used in early contributions may be subject to uncertainty owing to the instrumentation used, the comparison in table 2 is confined to the mean length

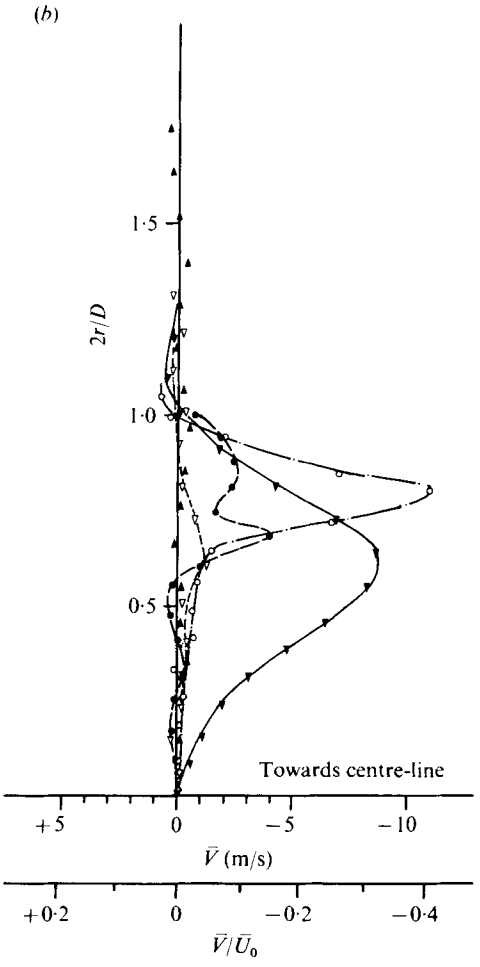

FIGURE 3. Radial profiles of (*a*) the axial and (*b*) the radial mean velocity in an annular jet. $\bar{U}_0$ = 26·8 m/s, D = 20·0 mm, d = 14·2 mm.

	●	○	▼	▽	▲	△	□
x/D	0·10	0·30	0·65	1·08	2·16	6·00	18·9
x/d	0·14	0·42	0·92	1·52	3·04	8·45	26·6

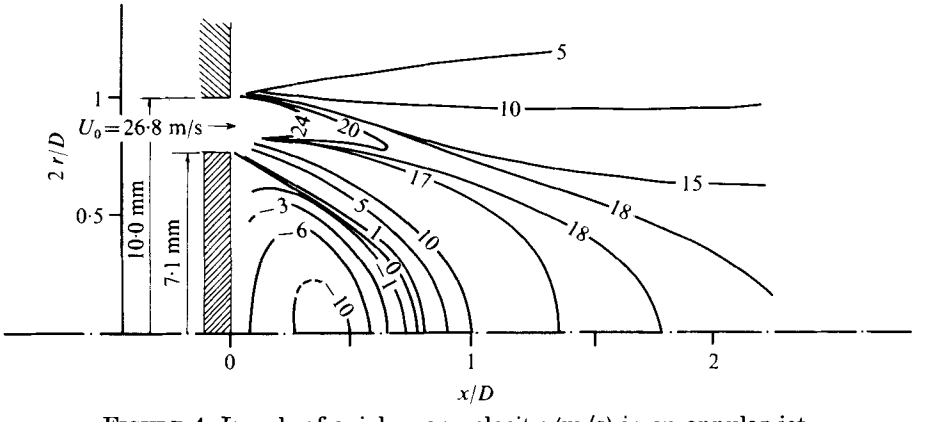

FIGURE 4. Isovels of axial mean velocity (m/s) in an annular jet.

Investigator(s)	Length of recirculation zone	Geometrical configuration
Nicholson & Field (1949)	$2d$–$3d$	Disk located inside a square duct
Carmody (1964)	$2{\cdot}5d$	Disk placed normal to a comparatively very large free stream of air
Chigier & Beér (1964)	$1{\cdot}10d$	Annular jet, $D = 97$ mm, $d/D = 0{\cdot}66$
Winterfeld (1965)	approx. $2d$ approx. independent of U approx. independent of d approx. independent of d^2/D^2 varying with obstacle shape	Disks placed in round tube, $D = 100$ mm
Davies & Beér (1971)	$1{\cdot}16d$ $1{\cdot}49d$ $2{\cdot}19d$	Annular jet, $D = 152{\cdot}4$ mm: $d/D = 0{\cdot}73$ $d/D = 0{\cdot}50$ $d/D = 0{\cdot}33$
Present investigation	$1{\cdot}00d$ $1{\cdot}15d$ $1{\cdot}45d$	Annular jet, $D = 20{\cdot}0$ mm: $d/D = 0{\cdot}71$ $d/D = 0{\cdot}62$ $d/D = 0{\cdot}44$

TABLE 2. Measured values of recirculation-zone length.

of the recirculation region. It shows that this length is strongly dependent on geometry and that, for the three investigations of annular jets, the agreement is good. The results of Davies & Beér (1971) suggest lengths which are approximately 15 % larger than the present results and those of Chigier & Beér (1964); discrepancies of this magnitude can probably arise from the detailed geometry of the annular jet. It should be emphasized that the centre-line location of zero instantaneous velocity varies with time and even at $x/d = 2{\cdot}0$ instantaneous negative velocities are still present; at the location of zero mean velocity the velocity probability distribution is nearly Gaussian as indicated in the following section.

4. Turbulence characteristics

The following discussion is concerned with the axial, radial and tangential normal stresses and the shear stress. The velocity probability density distributions, the corresponding skewness and flatness factors, and the turbulence energy spectra are presented.

Figures 5 and 6 present the normal stresses, normalized with the initial mean axial velocity, and correspond to the mean-velocity results in figures 2 and 3. The centre-line distributions in figure 5 show, in common with the mean values, a dependence upon the disk diameter but not upon the initial velocity; the tendency is for the axial normal stress to increase with decreasing disk diameter. In general, the turbulence is strongly anisotropic and only in the immediate vicinity of the disk and far downstream are the fluctuating components of similar magnitude.

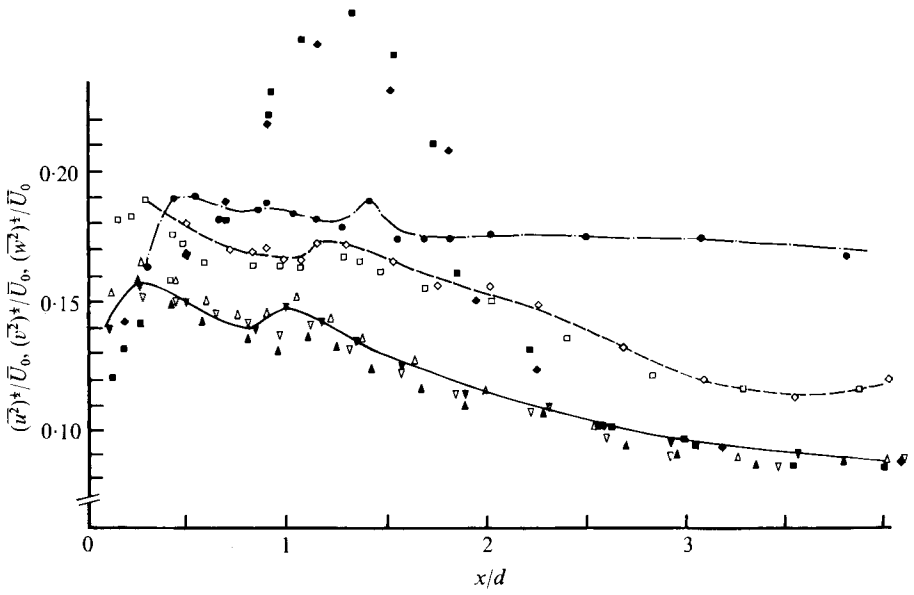

FIGURE 5. Centre-line profiles of the axial and radial normal stresses in an annular jet. D = 20·0 mm.

	$(\overline{u^2})^{\frac{1}{2}}$							$(\overline{v^2})^{\frac{1}{2}}$, $(\overline{w^2})^{\frac{1}{2}}$	
	●	◇	□	▼	▲	▽	△	◆	■
d (mm)	8·9	12·5	12·5	14·2	14·2	14·2	14·2	14·2	14·2
$\bar{U}_0$ (m/s)	39·5	39·5	26·8	39·5	26·8	16·9	9·4	39·5	26·8

In a large region around the mean stagnation point, i.e. $0{\cdot}4 \lesssim x/D \lesssim 2{\cdot}3$, the radial velocity fluctuations are much larger than the axial fluctuations (more than double at some locations), confirming the considerable influence of the radial velocity on the turbulent mixing process. The maximum value of the radial fluctuations occurs near where the mean velocity profile has an inflexion point while the profile of the axial fluctuations has two kinks located close to the disk and to the stagnation point respectively. In the recirculating region, the turbulence intensity is never less than around 0·3; further downstream, it has a minimum value of around 0·15 in the zone where the maximum centre-line mean velocity is located.

Figures 6(*a*), (*b*) and (*c*) present radial profiles of the axial, radial and tangential normal stresses, respectively, obtained with the largest disk and an initial velocity of 26·8 m/s. In the recirculation region, in spite of the decrease in the magnitude of the mean axial velocity, the axial stress increases from the centre-line to the edge, where small discontinuities appear. Outside this region, the axial fluctuations continue to increase rapidly in the radial direction, reach a maximum value then, at still larger radii, fall to a minimum close to the location of maximum mean velocity, which increases very rapidly with downstream distance. Closer to the edge of the jet, the stress increases again to a second maximum and finally decays slowly. The minimum turbulence intensity, in the recirculation region, is again around 0·3 and this readily accounts for the quantitative differences between the present results and those of Davies & Beér (1971), who measured with a hot-wire anemometer with consequent errors.

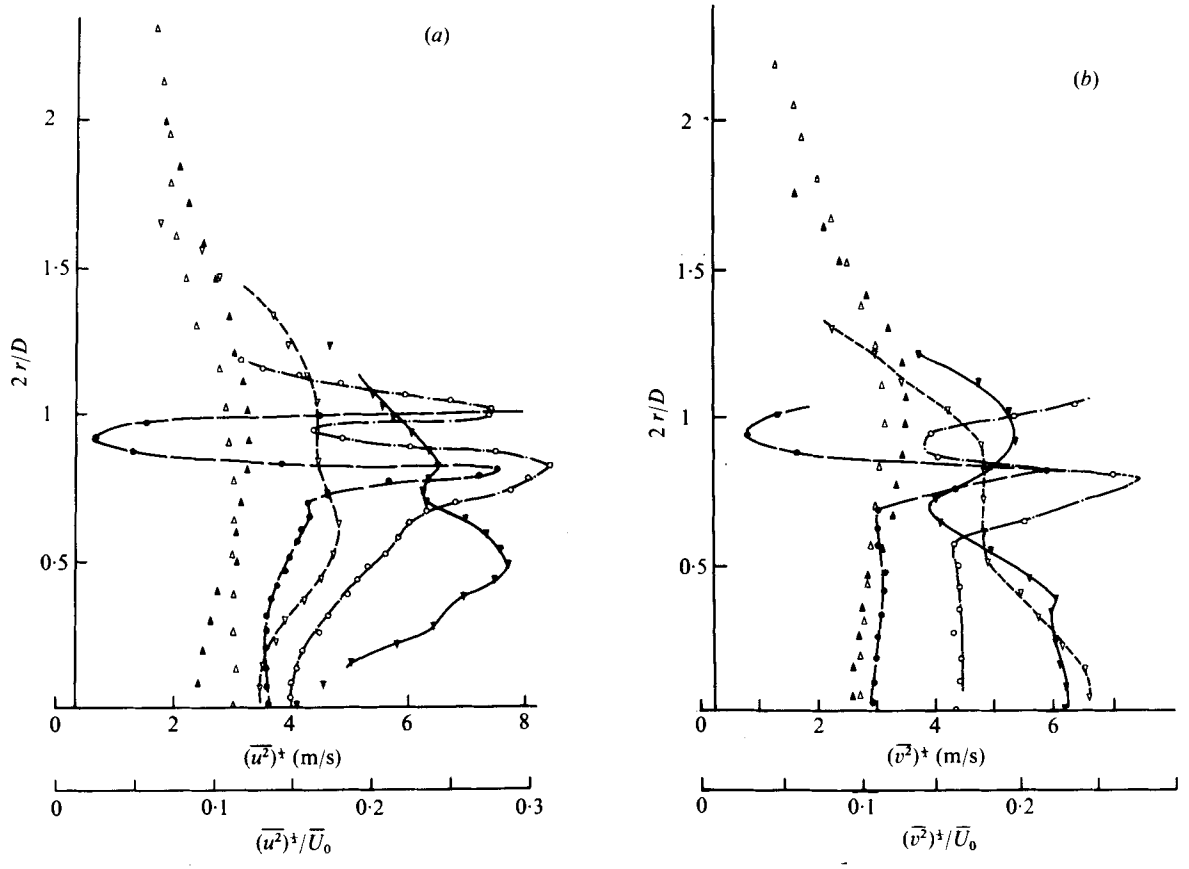

FIGURES 6 (*a*, *b*). For legend see opposite.

In contrast to the axial normal stress, the radial and tangential stresses do not exhibit the same increase from the centre-line to the edge of the recirculation region, and in some cases tend to decrease. Further from the centre-line, the general behaviour of all the normal stresses is similar although their magnitudes differ and the locations of the maxima and minima are not coincident. In contrast to the axial fluctuations, at $x/d = 1{\cdot}52$ the maximum of the r.m.s. radial and tangential fluctuations occurs at the centre-line.

Downstream of the recirculation region, the three normal stresses tend to diminish and the two maxima cannot be identified at $x/d = 3{\cdot}04$, where the centre-line values of the turbulence intensities reach their minima. At $x/d = 8{\cdot}45$ ($x/D = 6$), the profiles are very close to those of a fully developed free jet.

From the normal-stress values presented in figures 5 and 6, the turbulent kinetic energy can readily be evaluated and is relevant to turbulence models which make use of the corresponding conservation equation. As can be seen, however, the present flow is far from isotropic and consideration of the transport of individual stresses is important except, perhaps, in the far-downstream region.

Measured values of the shear stress are indicated on figure 7 and were obtained by subtracting measurements made with the fringes of the control volume inclined at

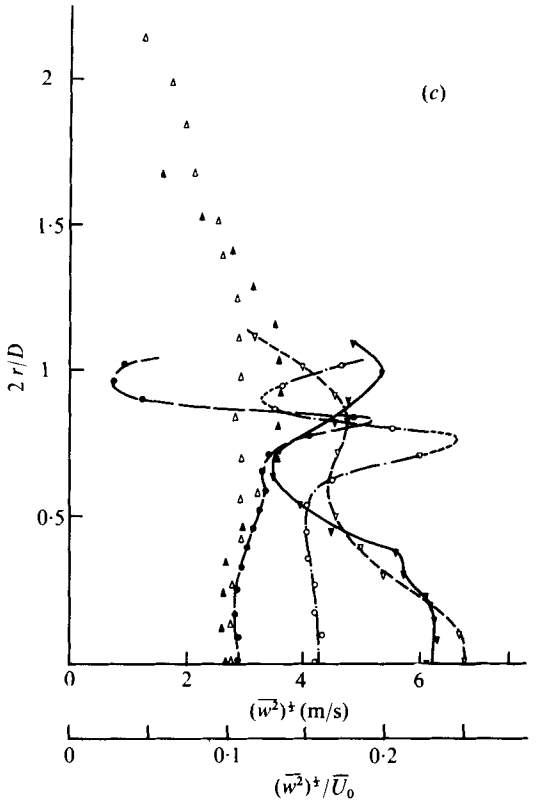

FIGURE 6. Radial profiles of (*a*) the axial, (*b*) the radial and (*c*) the tangential normal stress in an annular jet. $\overline{U}_0 = 26{\cdot}8$ m/s, $D = 20{\cdot}0$ mm, $d = 14{\cdot}2$ mm. Symbols as in figure 3.

$\pm 45°$ to the downstream direction: Durst, Melling & Whitelaw (1976, p. 348) provide further information on the related procedure. The profiles show the expected regions of negative shear, which remain until the regions of negative mean velocity have disappeared. Comparison of figures 3, 6 and 7 shows that the regions of zero shear do not, in general, correspond to those of zero velocity gradient or kinetic energy; this confirms the inability of effective-viscosity turbulence models to represent the flow characteristics and accounts for the emphasis on the use of Reynolds-stress closures by Pope & Whitelaw. The general anisotropy of the flow also suggests the need to consider each of the normal stresses individually. At downstream distances of around $6D$ and greater, near-equilibrium has been established and eddy-viscosity models may be more appropriate.

The experimental technique allowed the determination of velocity probability distributions and, therefore, of skewness and flatness factors. Along the centre-line the corresponding values were close to zero and three respectively and indicated the near-Gaussian nature of the axial and radial fluctuations. Figure 8 presents some of the centre-line distributions for the two velocity components and tabulates the related skewness and flatness factors, whose Gaussian nature suggests an absence of discrete frequencies. Such a near-Gaussian distribution exists along the centre-line of a free jet as reported by Ribeiro & Whitelaw (1975) and the present measurements show that

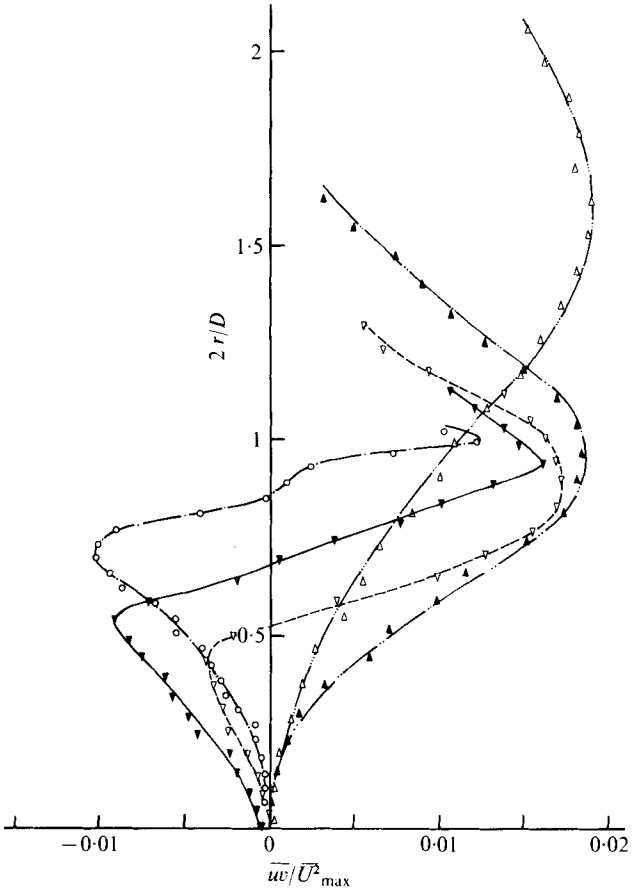

FIGURE 7. Radial profiles of the shear stress in an annular jet. $\overline{U}_0 = 26{\cdot}8$ m/s, $D = 20{\cdot}0$ mm, $d = 14{\cdot}2$ mm.

	○	▼	▽	▲	△
x/D	0·30	0·65	1·08	2·16	6·00
$\overline{U}_{max}$	24·1	19·9	19·1	18·9	12·5

the instantaneous variation of the velocity vector's direction does not significantly modify the symmetry of the combined (U, V) probability distribution.

The probability density distributions and correlations determined at all the measurement stations of the earlier figures, and discussed by Durão (1976), show that, in the region of recirculation, the probability distributions of the three velocity components are also nearly Gaussian. Close to the edges of the annular jet and in the core of the annular jet, however, the same is not true as indicated by figures 9 and 10, which present probability distributions of the axial velocity and of the radial and tangential velocities, respectively, as a function of radius at $x/D = 0{\cdot}1$. The corresponding tables show large values of the skewness and flatness factors, with rapid changes in the sign of the former, in the vicinity of the shear layers. Near the inside edge of the jet the distributions tend to become skewed towards lower velocities; this characteristic is magnified in the jet core, where the flatness factors assume the high values associated with spiky velocity characteristics and probability distributions with long tails.

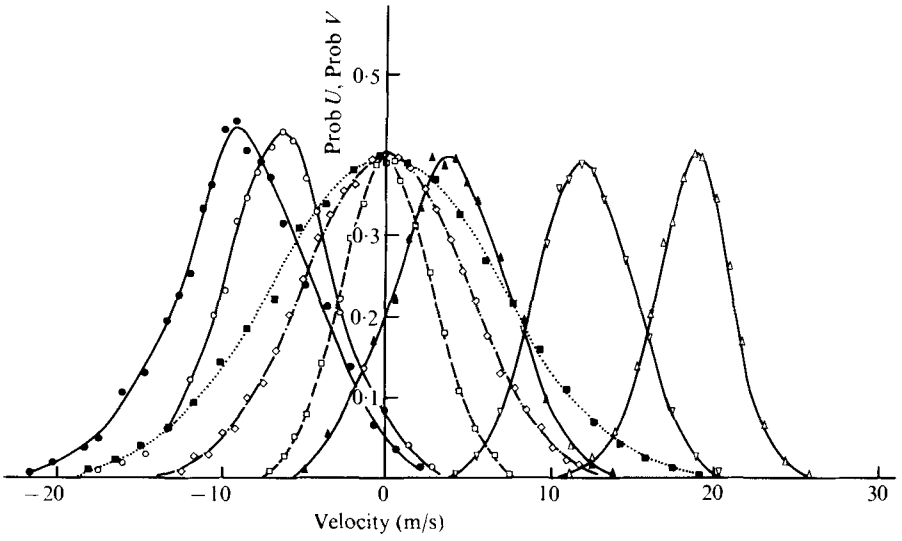

FIGURE 8. Velocity probability distributions of the axial and radial velocity components obtained along the centre-line of an annular jet. $\bar{U}_0 = 26{\cdot}8$ m/s, $D = 20{\cdot}0$ mm, $d = 14{\cdot}2$ mm.

	U					*V*		
	●	○	▲	△	▽	◇	■	□
x/D	0·19	0·56	0·80	2·41	6·30	0·48	0·94	1·88
$\bar{U}$ (m/s)	−8·70	−6·36	3·95	18·57	12·09	—	—	—
$(\overline{u^2})^{\frac{1}{2}}$ or $(\overline{v^2})^{\frac{1}{2}}$ (m/s)	4·26	3·62	3·45	2·27	2·90	4·80	6·83	2·81
Skewness	−0·07	−0·02	−0·02	−0·14	0·05	0·02	0·04	0·01
Flatness	2·93	3·19	2·76	2·99	2·74	3·12	3·03	2·94

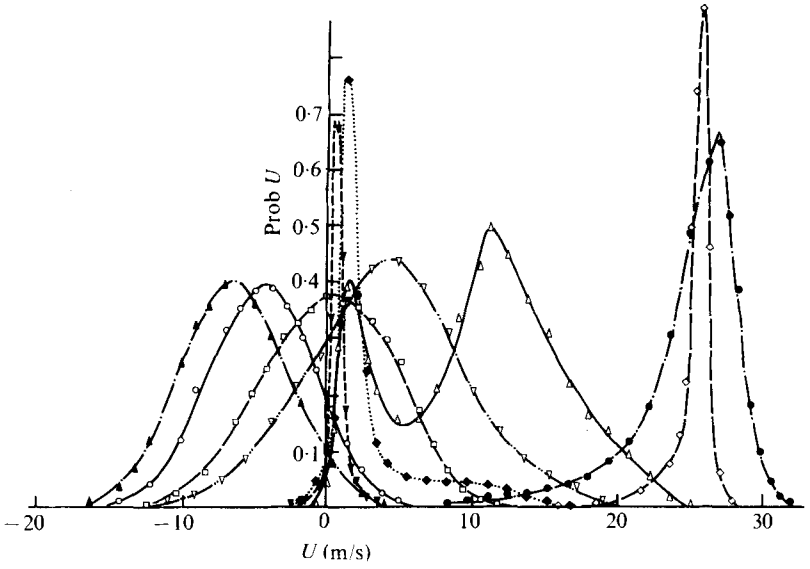

FIGURE 9. Velocity probability distributions of the axial velocity component obtained at different radii in an annular jet. $\bar{U}_0 = 26{\cdot}8$ m/s, $D = 20{\cdot}0$ mm, $d = 14{\cdot}2$, $x/D = 0{\cdot}1$.

	– – –, ▼	····, ◆	——, △	——, ◇	—·—, ●	—··—, ▽	——, □	——, ○	—·—, ▲
$2r/D$	1·04	1·02	1·01	0·97	0·83	0·76	0·69	0·36	0·01
$\bar{U}$ (m/s)	0·78	2·23	10·35	25·26	24·83	4·37	0·10	−6·44	−6·40
$(\overline{u^2})^{\frac{1}{2}}/\bar{U}$	15·10	1·33	0·54	0·06	0·15	1·30	35·95	0·85	0·57
Skewness	−0·42	2·23	−0·06	−2·87	−1·58	0·25	−0·16	0·09	0·03
Flatness	7·49	7·41	13·53	6·20	6·06	3·41	2·69	2·85	2·85

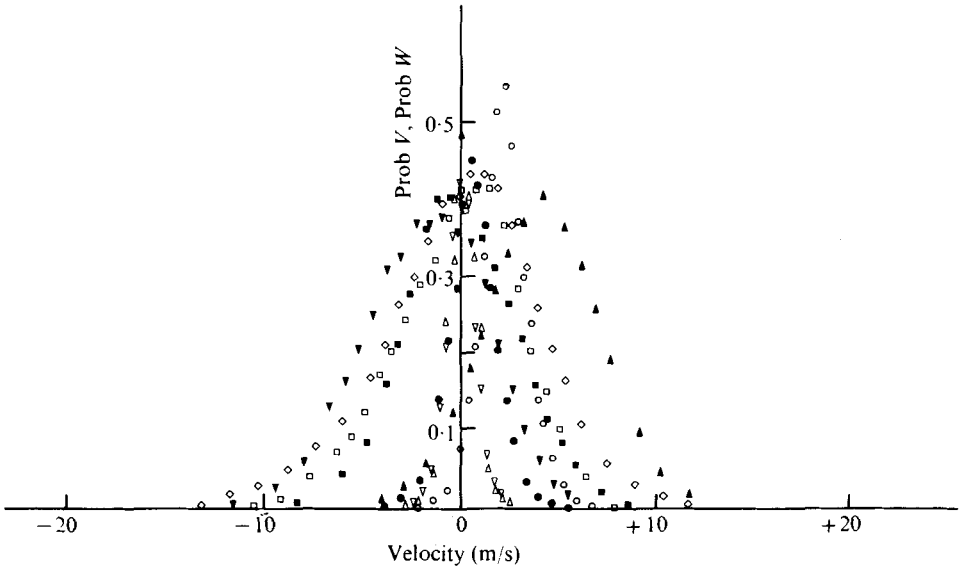

FIGURE 10. Velocity probability distributions of the radial and tangential velocity components obtained at different radii in an annular jet. $\bar{U}_0 = 26{\cdot}8$ m/s, $D = 20{\cdot}0$ mm, $d = 14{\cdot}2$ mm, $x/D = 0{\cdot}1$.

	W component					V component			
	■	□	◇	△	▽	▼	▲	○	●
$2r/D$	0·33	0·65	0·78	0·97	1·03	0·33	0·68	0·87	1·00
$\bar{V}$ (m/s)	—	—	—	—	—	−1·70	4·02	2·42	0·83
$(\overline{w^2})^{\frac{1}{2}}$ or $(\overline{v^2})^{\frac{1}{2}}$ (m/s)	2·95	3·29	4·15	0·80	0·99	3·08	3·02	1·65	1·26
Skewness	0·13	−0·25	−0·22	−0·35	0·01	−0·08	−0·01	0·25	0·55
Flatness	2·85	3·00	3·12	6·30	3·50	2·79	3·10	6·93	4·00

The spiky distribution corresponds to a low turbulence intensity due to the upstream contraction and the negative skewness reveals the influence, in the core of the jet, of the turbulent mixing caused by the recirculation behind the disk. A combined analysis of the probability distributions of U and V indicates that in this region of the flow, axial velocities larger than the mean velocity are more frequently associated with inward V components. The shear stress is therefore positive. In general, where deviations from Gaussian behaviour exist, they are greatest in the case of the axial velocity component. They tended to disappear with downstream distance but spiky distributions could still be observed at $x/D = 0{\cdot}3$.

Close to the outer edge of the jet, the probability distributions in figure 9 take on the bimodal form associated with the existence of a predominant frequency. At larger radii, the bimodal characteristic gives way to large positive skewness before returning towards Gaussian. This positive skewness of U is certainly associated with positive skewness of the V component, as discussed by Ribeiro & Whitelaw, and with positive values of $\overline{uv}$. Close to the exit, the entrainment in a round jet causes a similar effect as visualized by Bradshaw, Ferriss & Johnson (1964). This bimodal characteristic, according to the measured distributions, did not propagate into the region of recirculation. This region of the flow, and the location of the bimodal probability distribution,

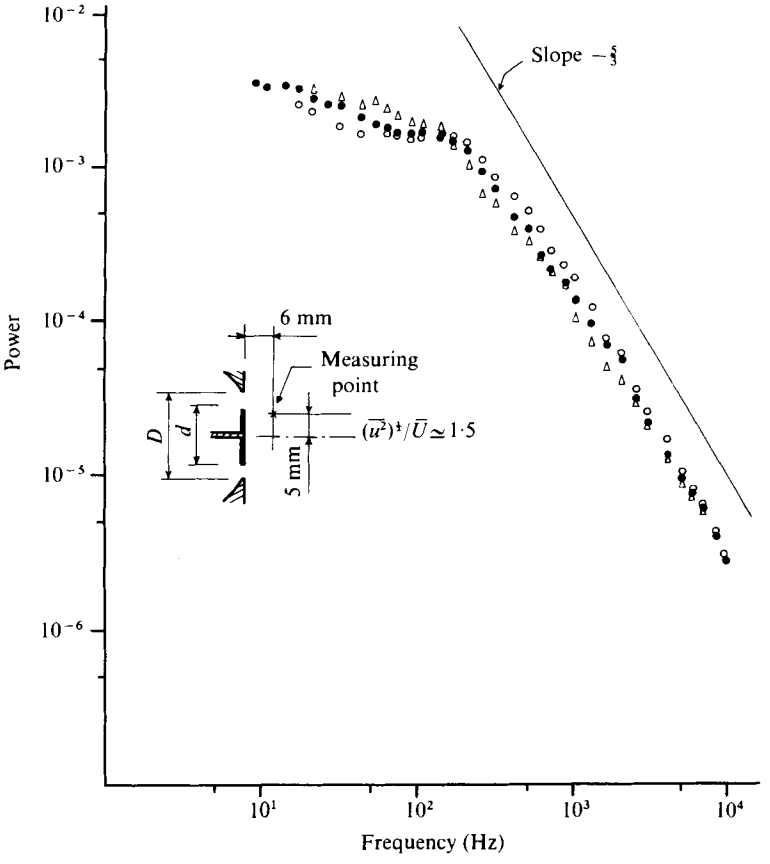

FIGURE 11. Turbulence spectra of axial velocity fluctuations. D = 20·0 mm, d = 14·2 mm. ○, $\overline{U}_0$ = 39·5 m/s; ●, $\overline{U}_0$ = 26·8 m/s; △, $\overline{U}_0$ = 16·9 m/s.

was examined in greater detail by frequency analysing the tracker demodulated signal corresponding to the axial velocity component. The Doppler signal, with the jet seeded with atomized silicone oil, was filtered (TTE type H71B), amplified (Hewlett Packard model 461A), mixed (Hatfield Instrument modulator type 1754) with a sine wave and filtered again (TTE type J61B or Harwell 95/2151) before being input to the Cambridge frequency-tracking demodulator. The demodulated signal was analysed with a type 1564-A General Radio sound and vibration analyser. A smaller beam angle was used to reduce the dynamic range of Doppler frequencies and the results obtained at $x/D = 3$ on the centre-line, where the turbulence intensity was approximately 15 %, were compared with those from a hot-wire anemometer; they were indistinguishable at frequencies up to 2 kHz.

Figure 11 shows turbulence energy spectra of the axial velocity component at $x/D = 0{\cdot}3$ and $2r/D = 0{\cdot}5$ for different initial velocities. This location is inside the recirculation region for all initial velocities and close to the region of zero mean velocity; the turbulence intensities are around 1·5. The turbulence energy has been normalized to have a total integrated energy equal to unity and the results show a slight influence of velocity in that they extend to higher frequencies with higher initial velocity. All spectra show a $-\frac{5}{3}$ region and are similar to those previously recorded, for example,

by Goldschmidt & Chuang (1972) in a round jet. A small spike may be present between 100 and 200 Hz but is insignificant compared with those observed close to the outer edge of the jet, where, corresponding to the bimodal probability distribution of figure 9, spectra were obtained with the hot-wire anemometer. The hot wire, which was sensitive to the axial and radial components, indicated predominant frequencies around 1·5 kHz but the total energy at the discrete frequencies was a small proportion of the total fluctuation energy. The presence of these predominant frequencies was linked to the outer shear layer of the jet and to values of x/D of 0·1; they were not observed in the recirculation region.

5. Conclusions

The following more important conclusions may be extracted from the preceding text:

(i) The curvature of the annular jet is dependent on the ratio of the inner to the outer diameter and increases with this ratio. Consequently, the length of the recirculation region normalized with disk diameter increases with decreasing disk diameter. The exit velocity does not have a significant influence on the length of the recirculation region at the higher velocities. The ratios of the maximum positive and negative centre-line velocities to the exit velocity increase with decreasing disk diameter and are essentially independent of the exit velocity.

(ii) The turbulent flow field is substantially anisotropic; over a large length of the centre-line, for example, the radial fluctuations are much larger than the axial fluctuations. The magnitude of the axial normal stresses inside the recirculation zone does not vary significantly and decreases downstream of the location of the stagnation point until the maximum mean velocity is obtained; subsequently, the flow develops in a manner similar to that for a free turbulent jet. The turbulence intensity in the recirculation region is very high with a minimum value of around 30 % along the centre-line. The initial velocity does not have a significant effect on the velocity fluctuations normalized with the initial velocity; in contrast, an increase in disk diameter results in a decrease in the intensity of the fluctuations.

(iii) The locations of zero shear stress do not coincide with those of zero mean velocity gradient. This behaviour suggests the need for Reynolds-stress closures in any turbulence model which is to represent the details of the flow. The anisotropy of the flow suggests that, in such turbulence models, the normal stresses must each be represented by conservation equations.

(iv) Close to the plane of the jet exit, and towards the outer edge of the annular jet, bimodal velocity probability distributions were measured and indicate that, in this region, a sine-wave type of oscillation is superimposed on the turbulence fluctuations. This behaviour has previously been observed in turbulent free jets. In contrast, the flow in the wake of the disk and particularly in the recirculation zone does not reveal bimodal distributions and measurements of turbulence energy spectra confirm the absence of predominant frequencies in this zone.

The authors are glad to acknowledge financial support from the Science Research Council.

REFERENCES

BAKER, R. J. 1974 The influence of particle seeding on laser anemometry measurements. *AERE* M-2644.

BRADSHAW, P., FERRISS, D. H. & JOHNSON, R. F. 1964 Turbulence in the noise-producing region of a circular jet. *J. Fluid Mech.* **19**, 591.

CARMODY, T. 1964 Establishment of the wake behind a disc. *J. Basic Engng, Trans. A.S.M.E.* **86**, 869.

CASTRO, I. P. & ROBINS, A. G. 1977 The flow around a surface-mounted cube in uniform and turbulent streams. *J. Fluid Mech.* **79**, 307.

CHIGIER, N. A. & BEÉR, J. M. 1964 The flow region near the nozzle in double concentric jets. *J. Basic Engng, Trans. A.S.M.E.* **86**, 797.

CLARE, H., DURÃO, D. F. G., MELLING, A. & WHITELAW, J. H. 1976 Investigation of a V-gutter stabilized flame by laser anemometry and schlieren photography. *Proc. AGARD Conf. Applications of Non-Intrusive Instrumentation in Fluid Flow Research, Saint-Louis*, paper 27.

DAVIES, T. W. & BEÉR, J. M. 1971 Flow in the wake of bluff-body flame stabilisers. *Proc. 13th Int. Symp. Combustion*, p. 637.

DURÃO, D. F. G. 1976 The application of laser anemometry to free jets and flames with and without recirculation. Ph.D. thesis, University of London.

DURÃO, D. F. G., LAKER, J. & WHITELAW, J. H. 1975 Digital processing of frequency-analysed Doppler signals. *Proc. LDA Symp. Accuracy of Flow Measurements by Laser Doppler Methods, Copenhagen*, p. 364.

DURÃO, D. F. G. & WHITELAW, J. H. 1974 Measurements in the region of recirculation behind a disc. *Proc. 2nd Int. Workshop on Laser Velocimetry, Purdue Univ.* vol. 2, p. 413. (See also *Técnica*, 1975, **426**, 297.)

DURÃO, D. F. G. & WHITELAW, J. H. 1975 The performance of acousto-optic cells for laser-Doppler anemometry. *J. Phys. E, Sci. Instrum.* **8**, 776.

DURÃO, D. F. G. & WHITELAW, J. H. 1976 Velocity characteristics of disc-stabilised diffusion and premixed flames. *Proc. A.I.A.A. Aerospace Sci. Meeting, Washington*, paper 76–34.

DURST, F., MELLING, A. & WHITELAW, J. H. 1976 *Principles and Practice of Laser-Doppler Anemometry*. Academic Press.

GOLDSCHMIDT, V. W. & CHUANG, S. C. 1972 Energy spectrum and turbulent scales in a circular water jet. *J. Basic Engng, Trans. A.S.M.E.* **94**, 22.

LONGWELL, J. P. 1953 Flame stabilization by bluff bodies and turbulent flames in ducts. *Proc. 4th Int. Symp. Combustion*, p. 90.

LONGWELL, J. P., CHENEVEY, J. E., CLARK, W. W. & FROST, E. E. 1949 Flame stabilization by baffles in a high velocity gas stream. *Proc. 3rd Symp. Combustion*, p. 40.

MELLING, A. 1975 Investigation of flow in non-circular ducts and other configurations by laser Doppler anemometry. Ph.D. thesis, University of London.

NICHOLSON, H. M. & FIELD, J. P. 1949 Some experimental techniques for the investigation of the mechanism of flame stabilization in the wake of bluff bodies. *Proc. 3rd Symp. Combustion*, p. 44.

POPE, S. B. & WHITELAW, J. H. 1976 The calculation of near-wake flows. *J. Fluid Mech.* **73**, 9.

RIBEIRO, M. M. & WHITELAW, J. H. 1975 Statistical characteristics of a turbulent jet. *J. Fluid Mech.* **70**, 1.

WINTERFELD, G. 1965 On processes of turbulent exchange behind flame holders. *Proc. 10th Int. Symp. Combustion*, p. 1265.

WOHL, K., KOPP, N. M. & GAZLEY, C. 1949 The stability of open flames. *Proc. 3rd Symp. Combustion*, p. 3.